北極域大気の起源解析

宮崎 和幸

国立研究開発法人　海洋研究開発機構

地球表層物質循環研究分野

地球環境観測研究開発センター

北極環境変動総合研究センター（UL: 滝川さん）

Arctic Air Pollution: Origins and Impacts

Kathy S. Law[1] and Andreas Stohl[2]

Notable warming trends have been observed in the Arctic. Although increased human-induced emissions of long-lived greenhouse gases are certainly the main driving factor, air pollutants, such as aerosols and ozone, are also important. Air pollutants are transported to the Arctic, primarily from Eurasia, leading to high concentrations in winter and spring (Arctic haze). Local ship emissions and summertime boreal forest fires may also be important pollution sources. Aerosols and ozone could be perturbing the radiative budget of the Arctic through processes specific to the region: Absorption of solar radiation by aerosols is enhanced by highly reflective snow and ice surfaces; deposition of light-absorbing aerosols on snow or ice can decrease surface albedo; and tropospheric ozone forcing may also be contributing to warming in this region. Future increases in pollutant emissions locally or in mid-latitudes could further accelerate global warming in the Arctic.
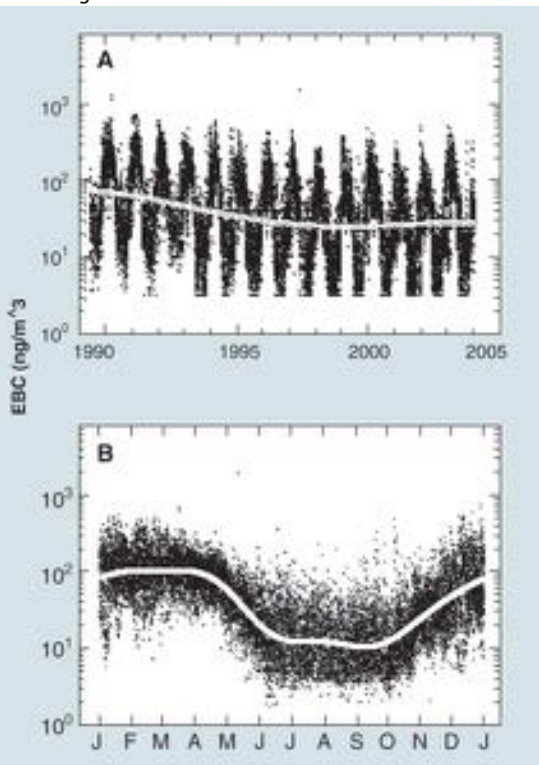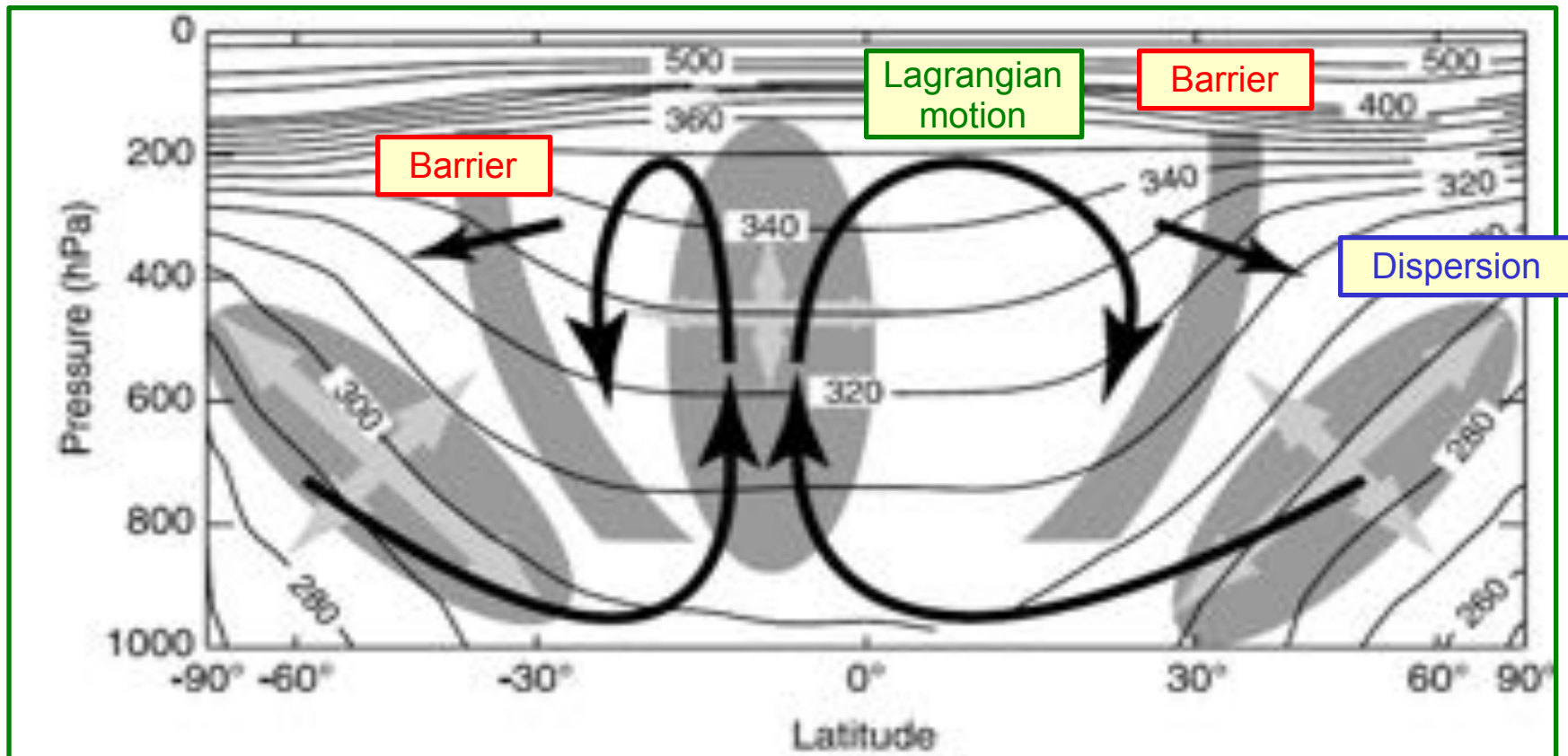

Fig. 1. Long-term trends (**A**) and seasonal variation (**B**) of 6-hourly equivalent BC concentrations at Alert. [Reproduced/ modified from (*10*) by permission of the American Geophysical

2-D Global-scale transport in the troposphere

K. Bowman

ARCTIC AIR POLLUTION
New Insights from POLARCAT-IPY

BY KATHARINE S. LAW, ANDREAS STOHL, PATRICIA K. QUINN,
CHARLES A. BROCK, JOHN F. BURKHART, JEAN-DANIEL PARIS,
GERARD ANCELLET, HANWANT B. SINGH, ANKE ROIGER, HANS SCHLAGER,
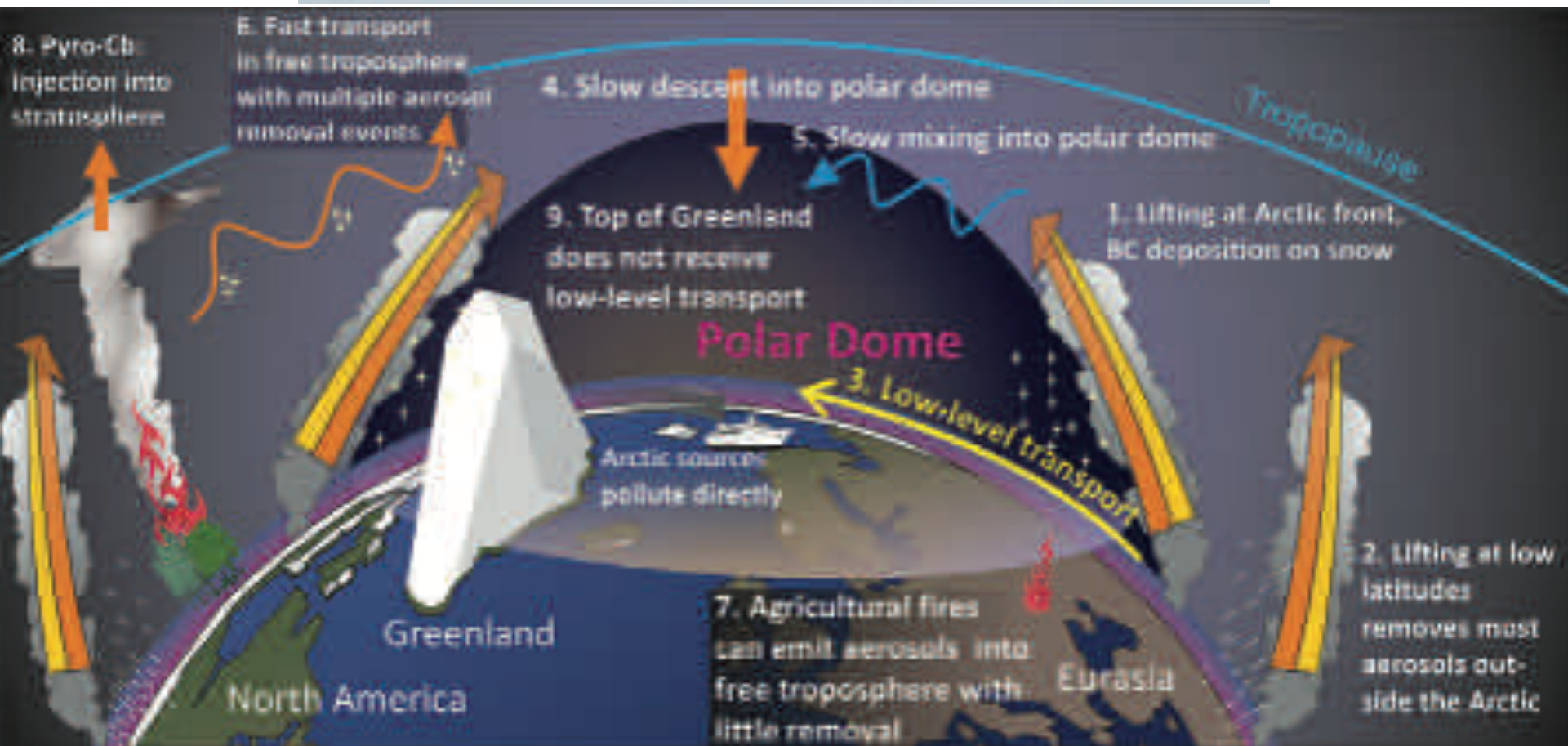JACK DIBB, DANIEL J. JACOB, STEVE R. ARNOLD, JACQUES PELON, AND JENNIE L. THOMAS

6

FIG. 2. Schematic showing pathways for the transport of air pollution into the

Airmass Origin in the Arctic. Part I: Seasonality

Clara Orbe,* Paul A. Newman,* Darryn W. Waugh,[+] Mark Holzer,[#,@] Luke D. Oman,* Feng Li,[&] and Lorenzo M. Polvani[#,**]

Laboratory for Atmospheric Chemistry and Dynamics, NASA Goddard Space Flight Center, Greenbelt, Maryland
[+]*Department of Earth and Planetary Sciences, Johns Hopkins University, Baltimore, Maryland*
[#]*Department of Applied Mathematics, School of Mathematics and Statistics, University of New South Wales, Sydney, New South Wales, Australia*
[@]*Department of Applied Physics and Applied Mathematics, Columbia University, New York, New York*
[&]*Goddard Earth Sciences Technology and Research, Universities Space Research Association, Columbia, Maryland*
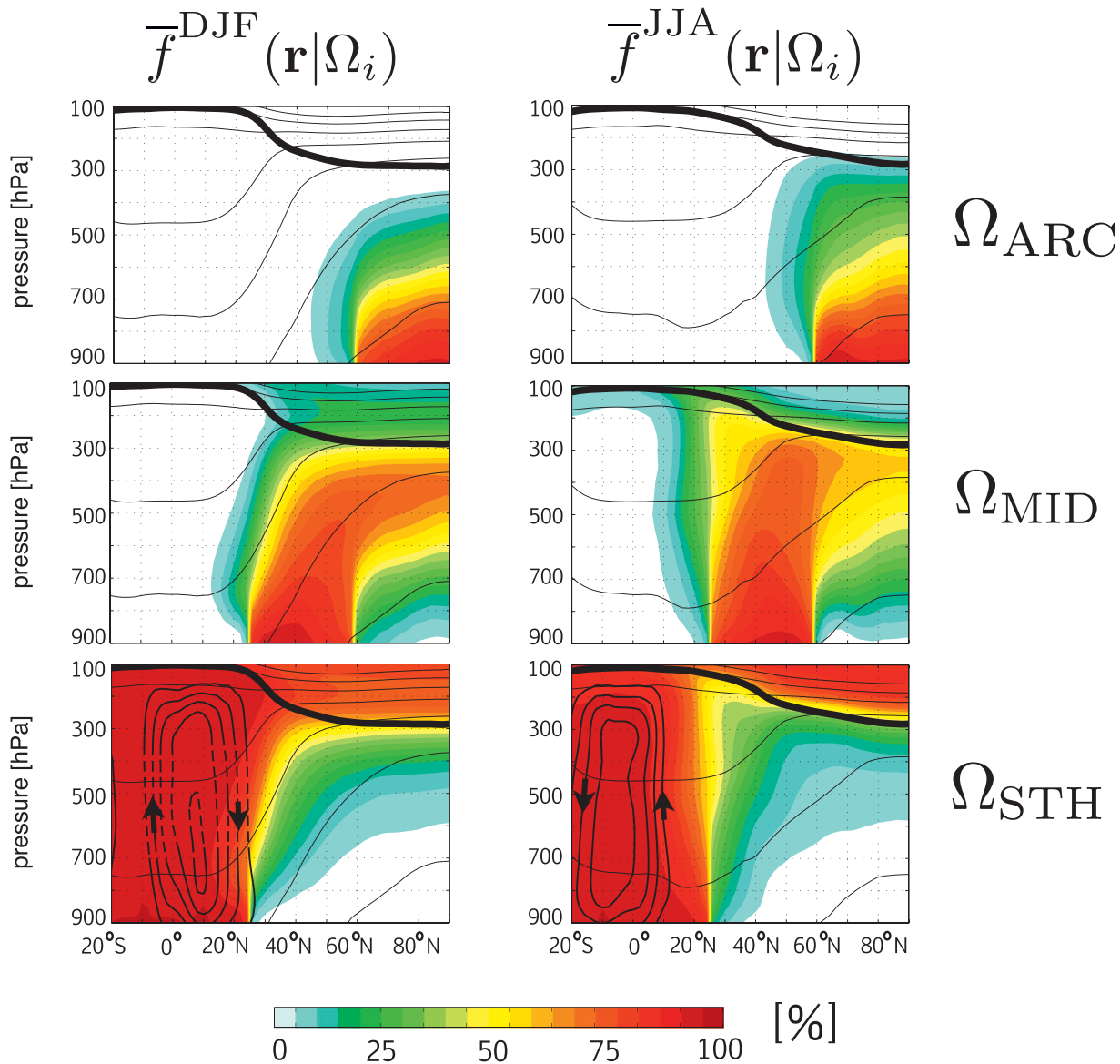**Lamont Doherty Earth Observatory, Columbia University, Palisades, New York*

FIG. 5. The fraction of air that last contacted the PBL over (top) Ω_{ARC}, (middle) Ω_{MID}, and (bottom) Ω_{STH}. DJF and JJA climatological mean airmass fractions $\overline{f}^{\mathrm{DJF}}(\mathbf{r}\,|\,\Omega_i)$ and $\overline{f}^{\mathrm{JJA}}(\mathbf{r}\,|\,\Omega_i)$ are shown in the left and right panels, respectively. The zonally averaged seasonal mean thermal tropopause is indicated by the thick black line. Seasonal mean isentropes are overlaid in black [20-K contour interval for isentropes between 270 and 390 K (DJF) and between 290 and 390 K (JJA)]. The mean streamfunction (contour interval: $60 \times 10^9\,\mathrm{kg\,s^{-1}}$) has also been overlaid on $\overline{f}^{\mathrm{DJF}}(\mathbf{r}\,|\,\Omega_{\mathrm{STH}})$ and $\overline{f}^{\mathrm{JJA}}(\mathbf{r}\,|\,\Omega_{\mathrm{STH}})$ in order to provide a sense for the zonally averaged tropospheric circulation in the tropics and subtropics.
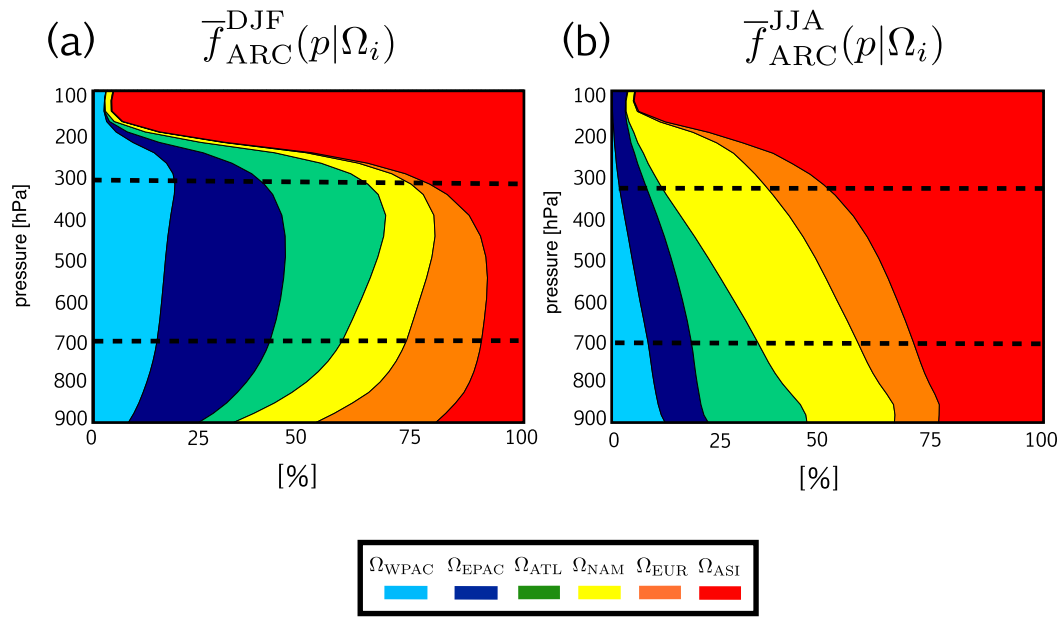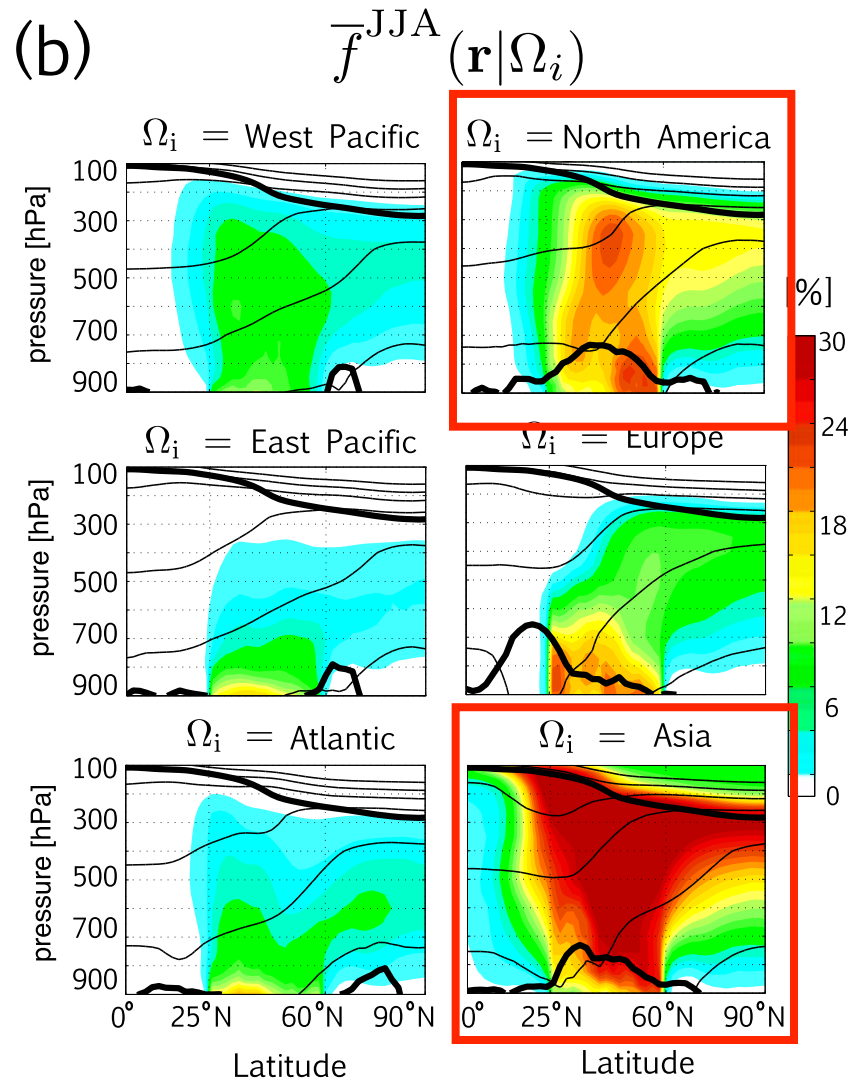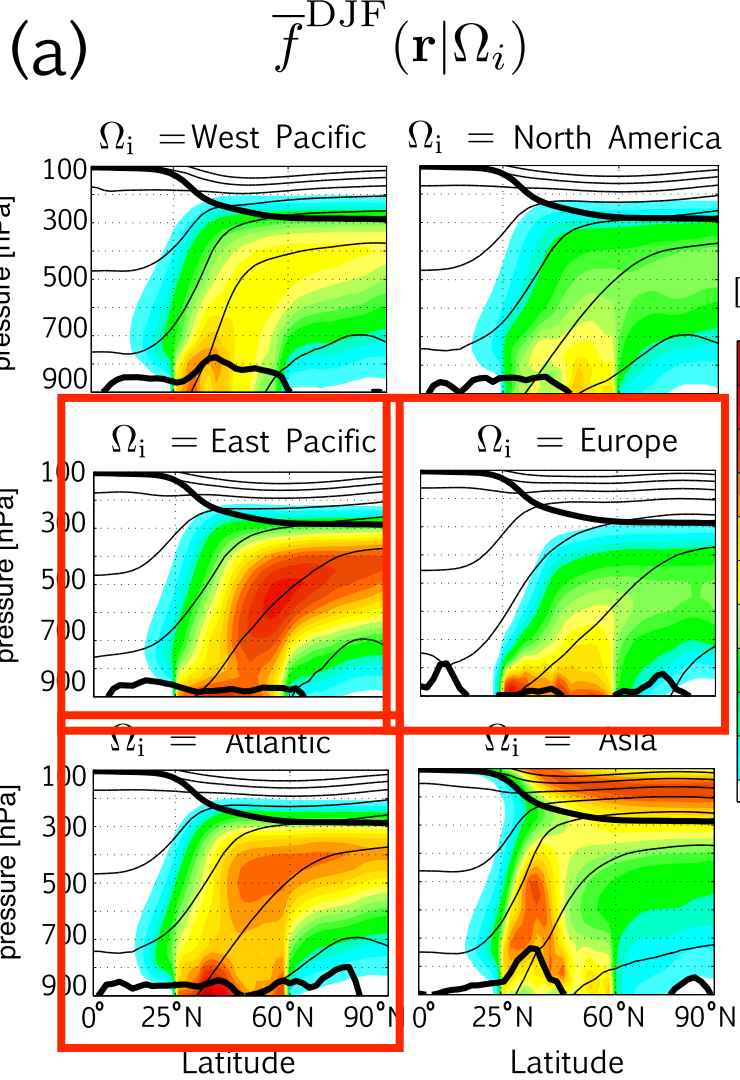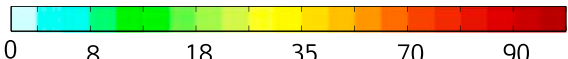
8

FIG. 6. (a) Vertical profiles of the DJF climatological mean airmass fractions in the Arctic that last contacted the PBL over the WPAC, EPAC, ATL, NAM, EUR, and ASI origin regions. Airmass fractions have been averaged over latitudes poleward of 60°N and normalized by the Arctic fraction that last had PBL contact over NH midlatitudes $\overline{f}_{\mathrm{ARC}}^{\mathrm{DJF}}(p\,|\,\Omega_{\mathrm{MID}})$, which during winter accounts for 51% ($\pm$2.2%) of the Arctic free troposphere (i.e., the 300–900-mb column integrated mass $\overline{f}^{\mathrm{DJF}}(\Omega)$; Table 1). (b) As in (a), but for JJA. The midlatitude airmass fraction in the normalization $\overline{f}_{\mathrm{ARC}}^{\mathrm{JJA}}(\Omega_{\mathrm{MID}})$ contributes 46% ($\pm$1.1%) of the total mass of the Arctic free troposphere during summer (Table 1).

TABLE 2. The DJF and JJA climatological mean fraction of the Arctic that last contacted the midlatitude PBL over the western Pacific, the eastern Pacific, the Atlantic, North America, Europe, and Asia. Airmass fractions corresponding to the Ω_i origin regions have been averaged over latitudes poleward of 60°N and column integrated over the free troposphere (300–900 mb; column 2), the lower troposphere (700–900 mb; column 3), and the middle-to-upper troposphere (300–700 mb; column 4). The denominators $\overline{f}_{\mathrm{ARC}}^{\mathrm{DJF}}(\Omega_{\mathrm{MID}})$ and $\overline{f}_{\mathrm{ARC}}^{\mathrm{JJA}}(\Omega_{\mathrm{MID}})$ correspond to the DJF and JJA climatological mean fraction of the Arctic that last contacted the PBL over NH midlatitudes.

PBL origin region Ω_i	Free troposphere, $\dfrac{\overline{\overline{f}}_{\mathrm{ARC}}(\Omega_i)}{\overline{\overline{f}}_{\mathrm{ARC}}(\Omega_{\mathrm{MID}})}$		Lower troposphere, $\dfrac{\overline{\overline{f}}_{\mathrm{ARC}}(\Omega_i)}{\overline{\overline{f}}_{\mathrm{ARC}}(\Omega_{\mathrm{MID}})}$		Middle troposphere, $\dfrac{\overline{\overline{f}}_{\mathrm{ARC}}(\Omega_i)}{\overline{\overline{f}}_{\mathrm{ARC}}(\Omega_{\mathrm{MID}})}$	
	DJF	JJA	DJF	JJA	DJF	JJA
WPAC	16%	9.1%	13%	10%	16%	9.0%
EPAC	26%	6.2%	25%	9.8%	26%	5.7%
ATL	20%	9.0%	15%	16%	21%	8.0%
NAM	13%	24%	16%	23%	12%	24%
EUR	13%	12%	20%	13%	12%	13%
ASI	12%	40%	12%	29%	12%	41%

9

(a) $\overline{f}^{\mathrm{DJF}}(\mathbf{r}|\Omega_i)$

$\Omega_i = $ West Pacific — $\Omega_i = $ North America — $\Omega_i = $ East Pacific — $\Omega_i = $ Europe — $\Omega_i = $ Atlantic — $\Omega_i = $ Asia

(b) $\overline{f}^{\mathrm{JJA}}(\mathbf{r}|\Omega_i)$

$\Omega_i = $ West Pacific — $\Omega_i = $ North America — $\Omega_i = $ East Pacific — $\Omega_i = $ Europe — $\Omega_i = $ Atlantic — $\Omega_i = $ Asia

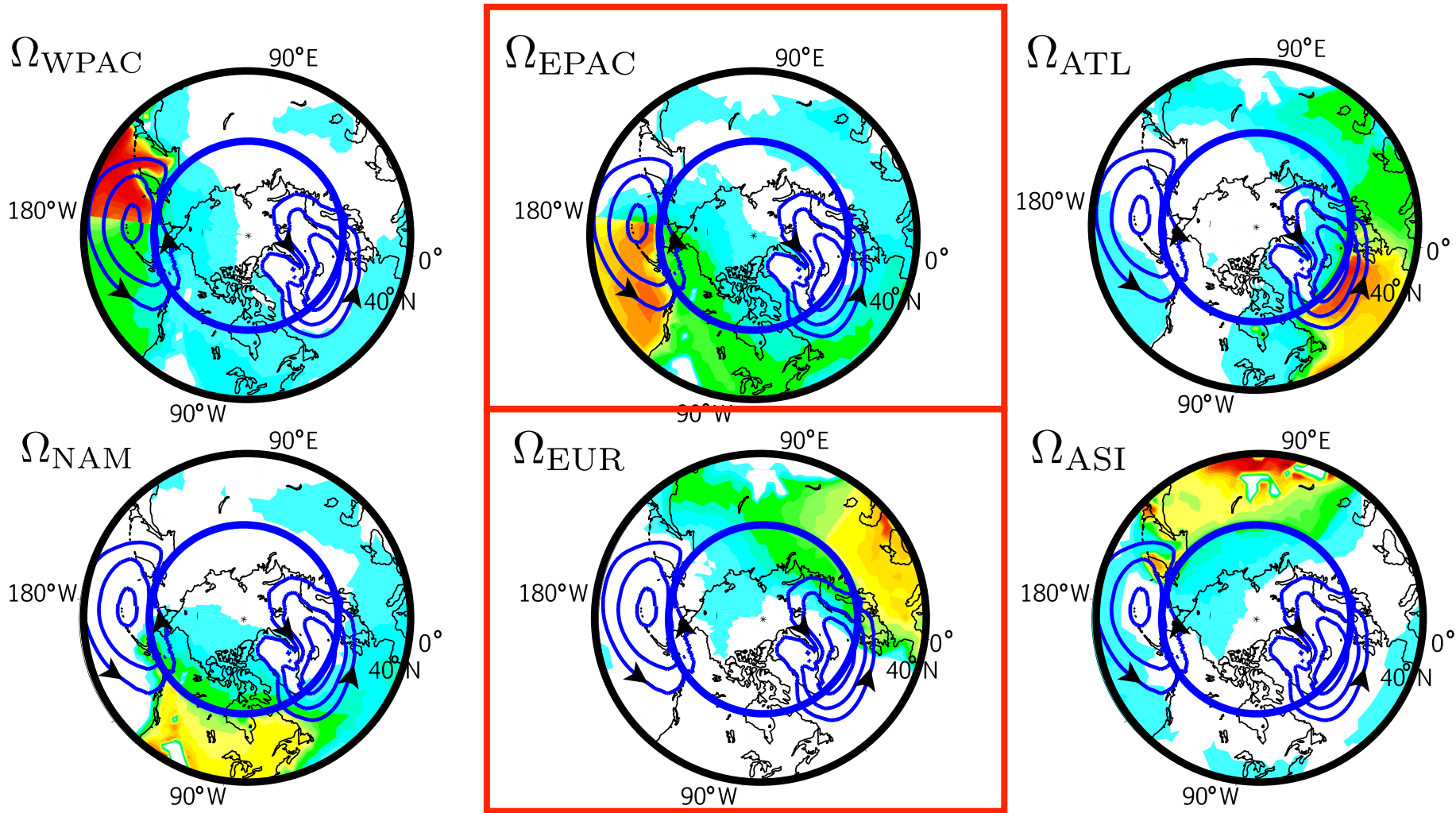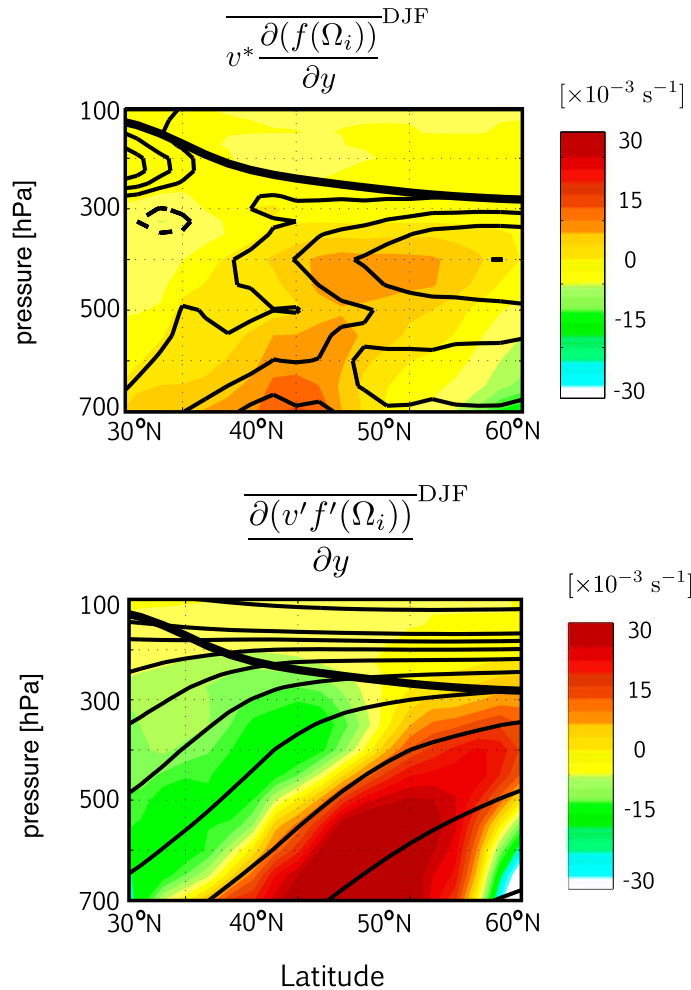| PBL origin region Ω_i	Free troposphere, $\dfrac{\overline{f}_{\mathrm{ARC}}(\Omega_i)}{\overline{f}_{\mathrm{ARC}}(\Omega_{\mathrm{MID}})}$		Lower troposphere, $\dfrac{\overline{f}_{\mathrm{ARC}}(\Omega_i)}{\overline{f}_{\mathrm{ARC}}(\Omega_{\mathrm{MID}})}$		Middle troposphere, $\dfrac{\overline{f}_{\mathrm{ARC}}(\Omega_i)}{\overline{f}_{\mathrm{ARC}}(\Omega_{\mathrm{MID}})}$	
	DJF	JJA	DJF	JJA	DJF	JJA
WPAC	16%	9.1%	13%	10%	16%	9.0%
EPAC	26%	6.2%	25%	9.8%	26%	5.7%
ATL	20%	9.0%	15%	16%	21%	8.0%
NAM	13%	24%	16%	23%	12%	24%
EUR	13%	12%	20%	13%	12%	13%
ASI	12%	40%	12%	29%	12%	41%

10

FIG. 8. The DJF climatological mean fraction of air at 800 mb that last contacted the midlatitude PBL over (top) the western Pacific, the eastern Pacific, and the Atlantic and (bottom) North America, Europe, and Asia, overlaid by the DJF mean sea level pressure (contours are shown for pressures between 980 and 996 mb; contour interval is 4 mb). Note that a nonlinear color bar has been used in order to highlight the spatial patterns of the Ω_i airmass fractions over the Arctic. In addition, recall that the sum of the six $\overline{f}^{\text{DJF}}(\mathbf{r}|\Omega_i)$ is $\overline{f}^{\text{DJF}}(\mathbf{r}|\Omega_{\text{MID}})$. The thick blue circle denotes the equatorward edge of Ω_{ARC} at 60°N.

(a) DJF Meridional Transport Terms for Ω_i = East Pacific

$$\overline{v^*\frac{\partial(f(\Omega_i))}{\partial y}}^{\text{DJF}}$$

$[\times 10^{-3}\ \text{s}^{-1}]$

30

15

0

−15

−30

pressure [hPa]

100 300 500 700

30°N 40°N 50°N 60°N

$$\overline{\frac{\partial(v'f'(\Omega_i))}{\partial y}}^{\text{DJF}}$$

$[\times 10^{-3}\ \text{s}^{-1}]$

30

15

0

−15

−30

pressure [hPa]

100 300 500 700

30°N 40°N 50°N 60°N

Latitude

(b) DJF Meridional Transport Terms Averaged Over [25°N–60°N]

pressure [hPa]

100 200 300 400 500 600 700 800

$$\overline{\left|\frac{\partial(v'f'(\Omega_i))}{\partial y}\right|}^{\text{DJF}}$$

$$\overline{\left|v^*\frac{\partial(f(\Omega_i))}{\partial y}\right|}^{\text{DJF}}$$

−5 0 5 10 15 20 25 30

$[\times 10^{-3}\ \text{s}^{-1}]$

Ω_i = East Pacific

Ω_i = Atlantic

Ω_i = West Pacific
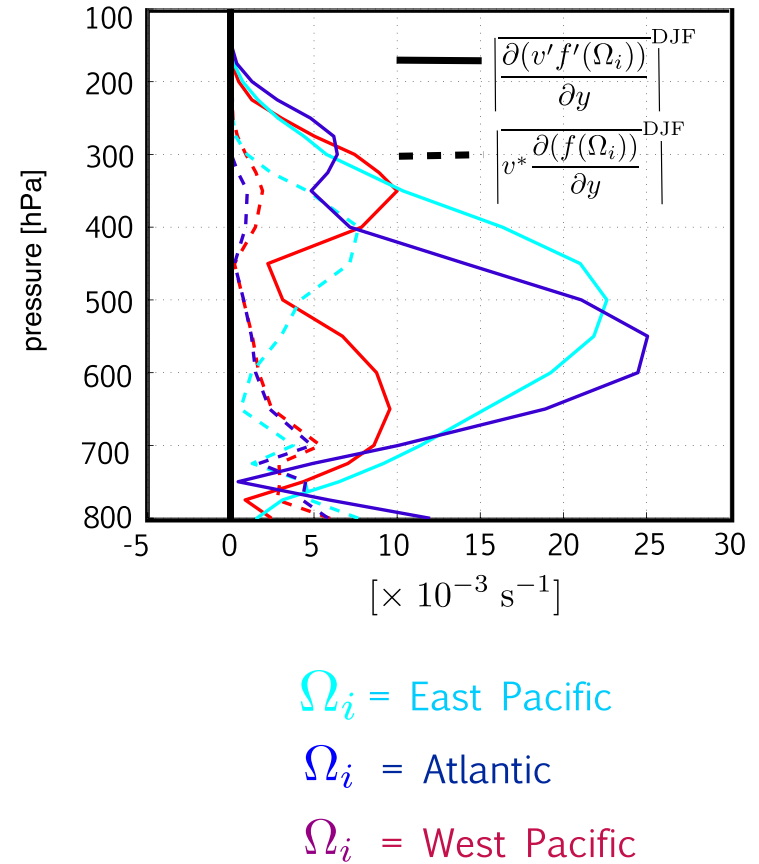
FIG. 10. (a) Comparison of the DJF climatological mean meridional advective- and eddy-induced transport terms (top) $\overline{v^*\partial(\Omega_i)/\partial y}^{\text{DJF}}$ and (bottom) $\overline{\partial v'f'(\Omega_i)/\partial y}^{\text{DJF}}$ for air that last contacted the PBL over the eastern Pacific. The DJF residual mean meridional velocity $\overline{v^*}^{\text{DJF}}$ is overlaid on the top panel with the black contours (contour interval: 0.3 m s^{-1}). DJF climatological mean isentropes are overlaid on the bottom panel with the black contours (contour interval: 10 K). The DJF mean thermal tropopause is indicated in both panels by the thick black line. (b) Comparison of the advective and eddy transport terms (dashed and solid lines respectively) for the airmass fractions that last contacted the PBL over the eastern Pacific (cyan), the Atlantic (blue), and the western Pacific (red). The transport terms have been averaged over the midlatitude origin region (i.e., latitudes 25°–60°N) and have been expressed in terms of their absolute magnitudes.

Air-mass Origin in the Arctic. Part II: Response to Increases in Greenhouse Gases

CLARA ORBE,* PAUL A. NEWMAN,* DARRYN W. WAUGH,[+] MARK HOLZER,[#,@] LUKE D. OMAN,* FENG LI,[&] AND LORENZO M. POLVANI[@,**]

*Laboratory for Atmospheric Chemistry and Dynamics, NASA Goddard Space Flight Center, Greenbelt, Maryland
[+] Department of Earth and Planetary Sciences, Johns Hopkins University, Baltimore, Maryland
[#] Department of Applied Mathematics, School of Mathematics and Statistics, University of New South Wales, Sydney, New South Wales, Australia
[@] Department of Applied Physics and Applied Mathematics, Columbia University, New York, New York
[&] Goddard Earth Sciences Technology and Research, Universities Space Research Association, Columbia, Maryland
**Lamont-Doherty Earth Observatory, Columbia University, Palisades, New York

Future changes in transport from Northern Hemisphere (NH) midlatitudes into the Arctic are examined using rigorously defined air-mass fractions that partition air in the Arctic according to where it last had contact with the planetary boundary layer (PBL). Boreal winter (December–February) and summer (June–August) air-mass fraction climatologies are calculated for the modeled climate of the Goddard Earth Observing System Chemistry–Climate Model (GEOSCCM) forced with the end-of-twenty-first century greenhouse gases and ozone-depleting substances. The modeled projections indicate that the fraction of air in the Arctic that last contacted the PBL over NH midlatitudes (or air of "midlatitude origin") will increase by about 10% in both winter and summer. The projected increases during winter are largest in the upper and middle Arctic troposphere, where they reflect an upward and poleward shift in the transient eddy meridional wind, a robust dynamical response among comprehensive climate models. The boreal winter response is dominated by (~5%–10%) increases in the air-mass fractions originating over the eastern Pacific and the Atlantic, while the response in boreal summer mainly reflects (~5%) increases in air of Asian and North American origin. The results herein suggest that future changes in transport from midlatitudes may impact the composition—and, hence, radiative budget—in the Arctic, independent of changes in emissions.

(a) $\Delta \overline{f}^{\mathrm{DJF}}(\mathbf{r}|\Omega_i)$ (b) $\Delta \overline{f}^{\mathrm{JJA}}(\mathbf{r}|\Omega_i)$

Ω_{ARC}

Ω_{MID}

Ω_{STH}

Latitude

[%]   [%]

15
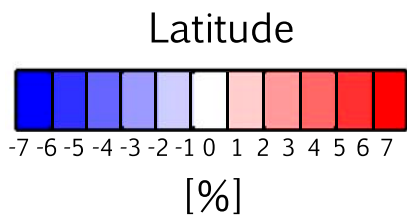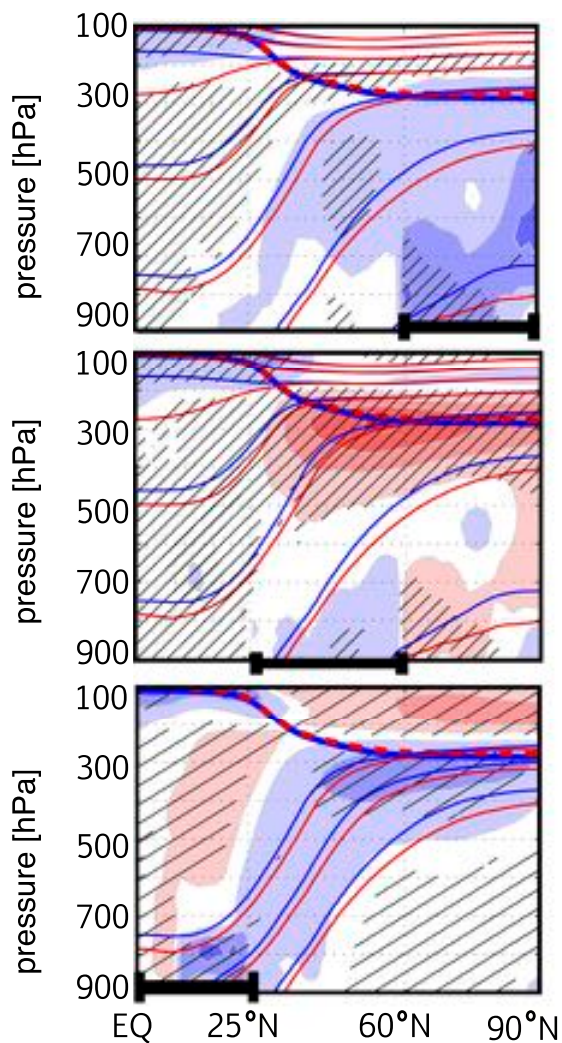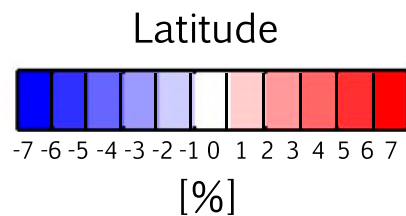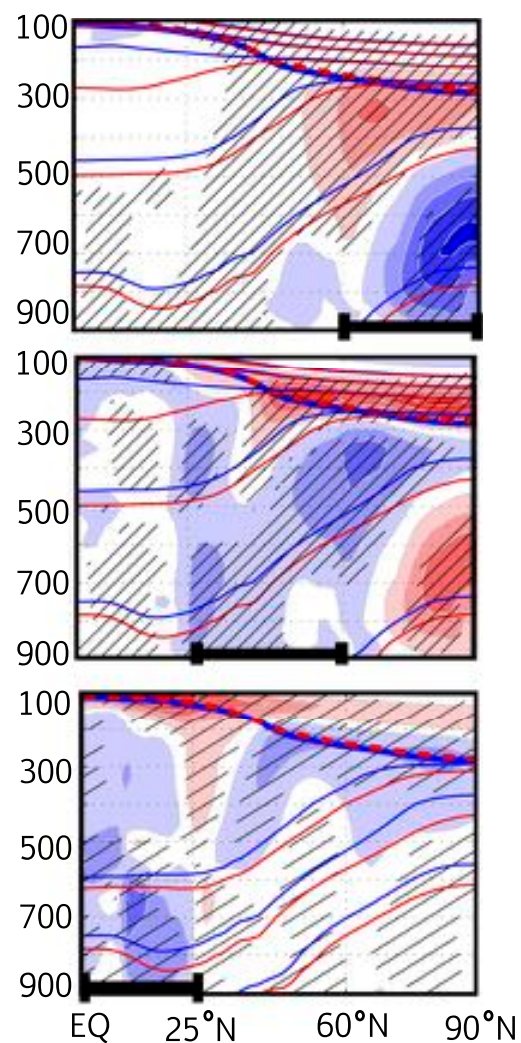
(a) $\Delta \overline{f}^{\mathrm{DJF}}(\mathbf{r}|\Omega_i)$

(b) $\Delta \overline{f}^{\mathrm{JJA}}(\mathbf{r}|\Omega_i)$
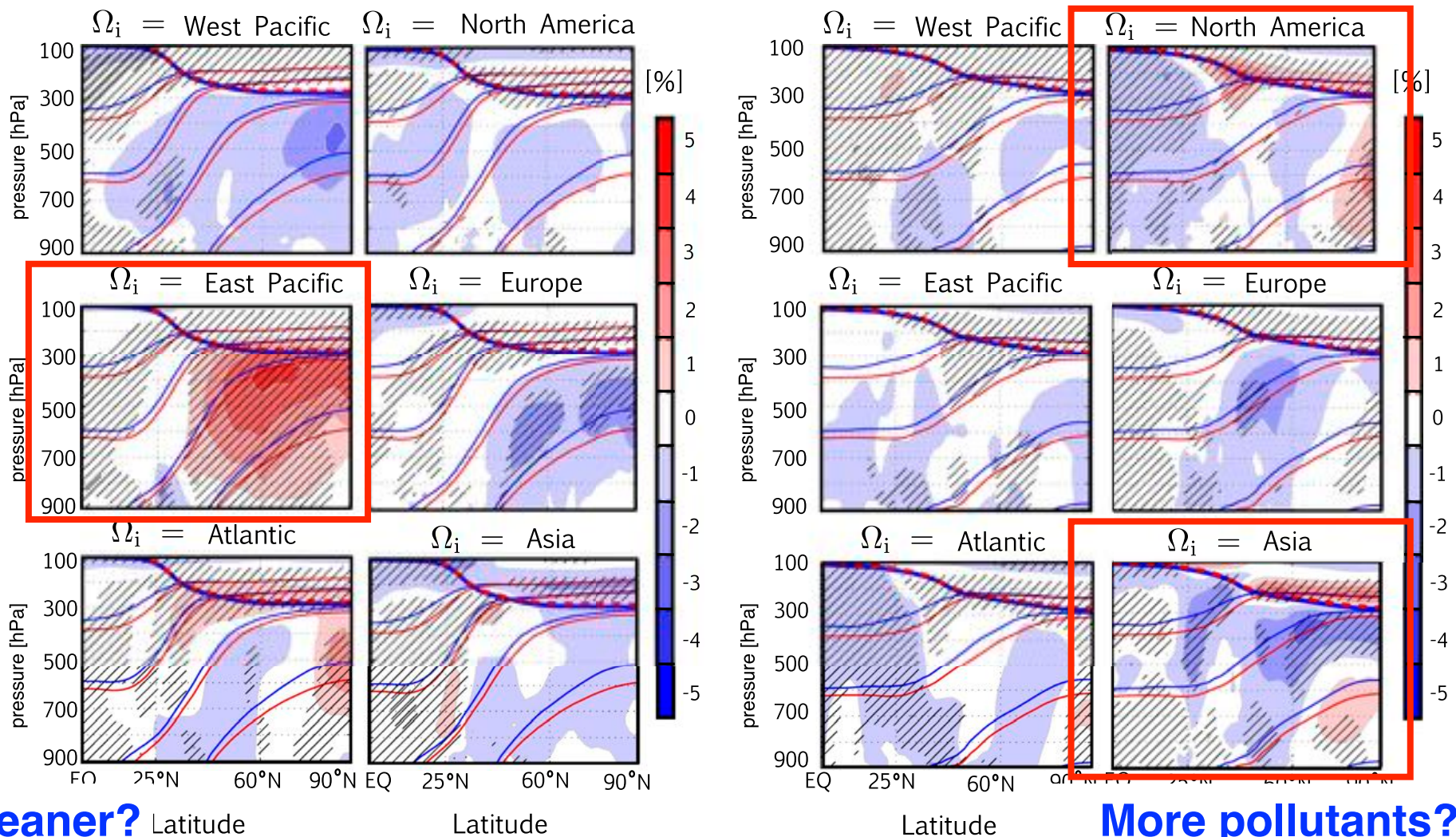
Cleaner? **More pollutants?**

FIG. 4. FTR − REF changes in the fraction of air that last contacted the PBL between 25° and 60°N (Ω_{MID}), further partitioned according to last contact (left) over ocean (i.e., the western Pacific, the eastern Pacific, the Atlantic) and (right) over land (i.e., North America, Europe, and Asia). Future changes (a) in the DJF climatological mean air-mass fractions $\Delta \overline{f}^{\mathrm{DJF}}(\mathbf{r}|\Omega_i)$ and (b) in the JJA climatological mean air-mass fractions $\Delta \overline{f}^{\mathrm{JJA}}(\mathbf{r}|\Omega_i)$ are shown. The zonally averaged seasonal mean thermal tropopause for the REF and FTR climates is indicated by the solid blue and dashed red lines, respectively. Seasonal-mean isentropes are overlaid with the thin blue and red lines for the REF and FTR climates, respectively (280–340 K, with contour interval of 20 K). Regions where the diagnosed climate changes are statistically significant at the 90% confidence level are shown with the gray hatching.

本年度の研究計画

解析データの作成:衛星観測をデータ同化したトップダウン解析により排出源情報を高度化し、一酸化炭素大気分布の再現実験を実施する。各種観測との比較からその性能を明らかにする。 **北極域への輸送解析における一酸化炭素の有用性を判断する。**

輸送診断手法の改良: 平均流輸送と渦混合への分離、断熱過程と非断熱過程への分離に加えて、**帯状平均構造から3次元構造へと拡張し、大気組成輸送の時空間構造に対して新解釈を与える**ことを検討する。

Tropospheric chemistry reanalysis data for the years 2005-2014: CHASER-EnKF

Tropospheric chemistry reanalysis data for the years 2005-2014: CHASER-EnKF
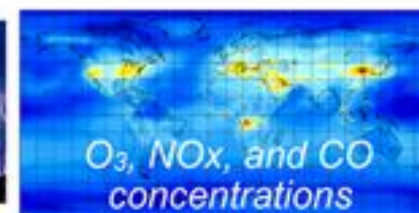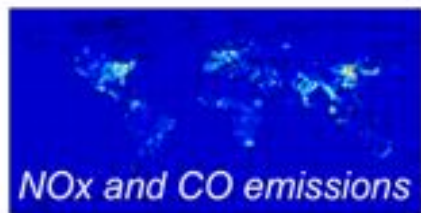
This web page provides a 10-year (2005-2014) global data set of the chemical concentrations of various species and emissions of several precursors for the period 2005-2014 estimated from a data assimilation of multiple satellite measurements (OMI, MLS, TES, and MOPITT).

O Short description

▸ Provide the results from a 10-year tropospheric chemistry reanalysis for the period 2005-2014 obtained by assimilating multiple data sets from the OMI, MLS, TES, and MOPITT satellite instruments. The reanalysis calculation was conducted using a global chemical transport model (CHASER) and an ensemble Kalman filter (EnKF) technique that simultaneously optimises the chemical concentrations of various species and emissions of several precursors. The optimisation of both the concentration and the emission fields is an efficient method to correct the entire tropospheric profile and its year-to-year variations, and to adjust various tracers chemically linked to the species assimilated.

▸ Comparisons against independent aircraft, satellite, and ozonesonde observations demonstrate the quality of the analysed O3, NO2, and CO concentrations on regional and global scales and for both seasonal and year- to-year variations from the lower troposphere to the lower stratosphere. The data assimilation statistics imply persistent reduction of model error and improved representation of emission variability, but

Data download

The reanalysis data are provided on T42 horizontal resolution (2.8 degree for longitude and the T42 Gaussian grid for latitude) and 22 pressure levels (1000, 995, 980, 950, 900, 850, 800, 750, 700, 600, 500, 400, 350, 300, 250, 100, 175, 150, 125, 100, 85, 70) in NetCDF format.

1. Monthly mean

	2005	2006	2007	2008	2009	2010	2011	2012	2013	2014
O3 (ppb)	o3_mon_2005.nc [8 MB]	o3_mon_2006.nc [8 MB]	o3_mon_2007.nc [8 MB]	o3_mon_2008.nc [8 MB]	o3_mon_2009.nc [8 MB]	o3_mon_2010.nc [8 MB]	o3_mon_2011.nc [8 MB]	o3_mon_2012.nc [8 MB]	o3_mon_2013.nc [8 MB]	o3_mon_2014.nc [8 MB]
CO (ppb)	co_mon_2005.nc [8 MB]	co_mon_2006.nc [8 MB]	co_mon_2007.nc [8 MB]	co_mon_2008.nc [8 MB]	co_mon_2009.nc [8 MB]	co_mon_2010.nc [8 MB]	co_mon_2011.nc [8 MB]	co_mon_2012.nc [8 MB]	co_mon_2013.nc [8 MB]	co_mon_2014.nc [8 MB]
NO2 (ppb)	no2_mon_2005.nc [8 MB]	no2_mon_2006.nc [8 MB]	no2_mon_2007.nc [8 MB]	no2_mon_2008.nc [8 MB]	no2_mon_2009.nc [8 MB]	no2_mon_2010.nc [8 MB]	no2_mon_2011.nc [8 MB]	no2_mon_2012.nc [8 MB]	no2_mon_2013.nc [8 MB]	no2_mon_2014.nc [8 MB]
Surface NOx emissions (kg m^{-2} s^{-1})	snox_mon_2005.nc [0.3 MB]	snox_mon_2006.nc [0.3 MB]	snox_mon_2007.nc [0.3 MB]	snox_mon_2008.nc [0.3 MB]	snox_mon_2009.nc [0.3 MB]	snox_mon_2010.nc [0.3 MB]	snox_mon_2011.nc [0.3 MB]	snox_mon_2012.nc [0.3 MB]	snox_mon_2013.nc [0.3 MB]	snox_mon_2014.nc [0.3 MB]
Surface CO emissions (kg m^{-2} s^{-1})	sco_mon_2005.nc [0.3 MB]	sco_mon_2006.nc [0.3 MB]	sco_mon_2007.nc [0.3 MB]	sco_mon_2008.nc [0.3 MB]	sco_mon_2009.nc [0.3 MB]	sco_mon_2010.nc [0.3 MB]	sco_mon_2011.nc [0.3 MB]	sco_mon_2012.nc [0.3 MB]	sco_mon_2013.nc [0.3 MB]	sco_mon_2014.nc [0.3 MB]
Lightning NOx sources (kg m^{-2} s^{-1})	lnox_mon_2005.nc [0.3 MB]	lnox_mon_2006.nc [0.3 MB]	lnox_mon_2007.nc [0.3 MB]	lnox_mon_2008.nc [0.3 MB]	lnox_mon_2009.nc [0.3 MB]	lnox_mon_2010.nc [0.3 MB]	lnox_mon_2011.nc [0.3 MB]	lnox_mon_2012.nc [0.3 MB]	lnox_mon_2013.nc [0.3 MB]	lnox_mon_2014.nc [0.3 MB]

Galleries
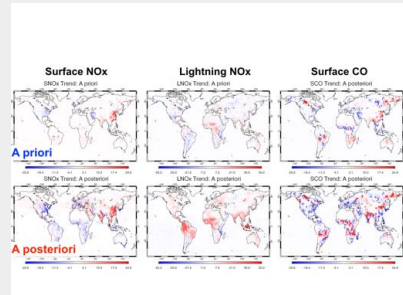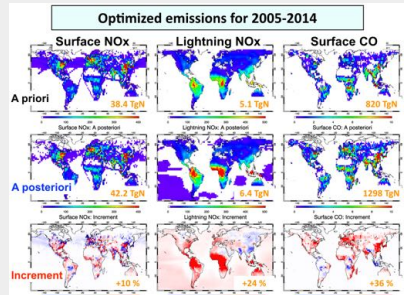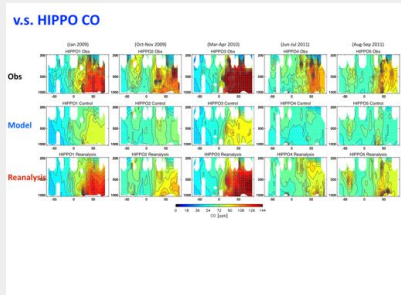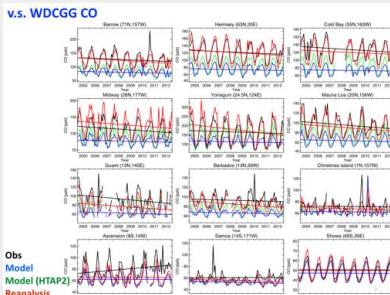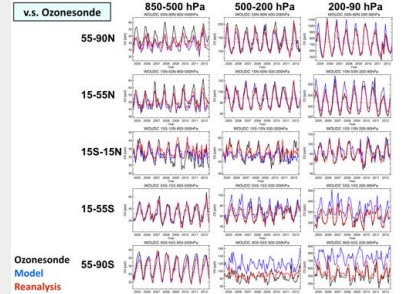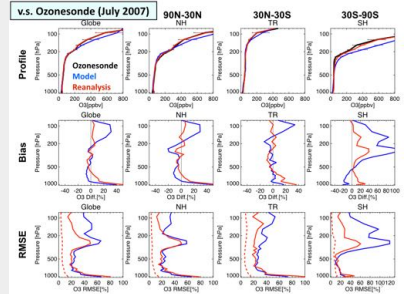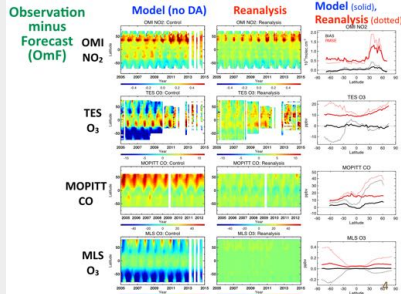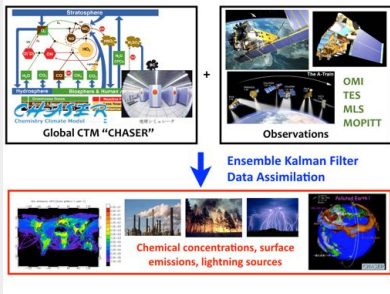
Contact information

Kazuyuki Miyazaki

(Japan Agency for Marine-Earth Science and Technology)

✉ kmiyazaki@jamstec.go.jpkmiyazaki@jamstec.go.jp

https://sites.google.com/site/kazuyukimiyazaki/

» DEGCR TOP　　» Research theme　　» Members　　» Activity Report　　» Databases

» Atmosphere
» Land
» Atmosphere-Ocean
　interaction
» Land-Atmosphere
　interaction

» [NEW]2nd (6th in total) DEGCR
　+ AGCR unit/IASC all meeting
» 1st (5th in total) DEGCR + AGCR
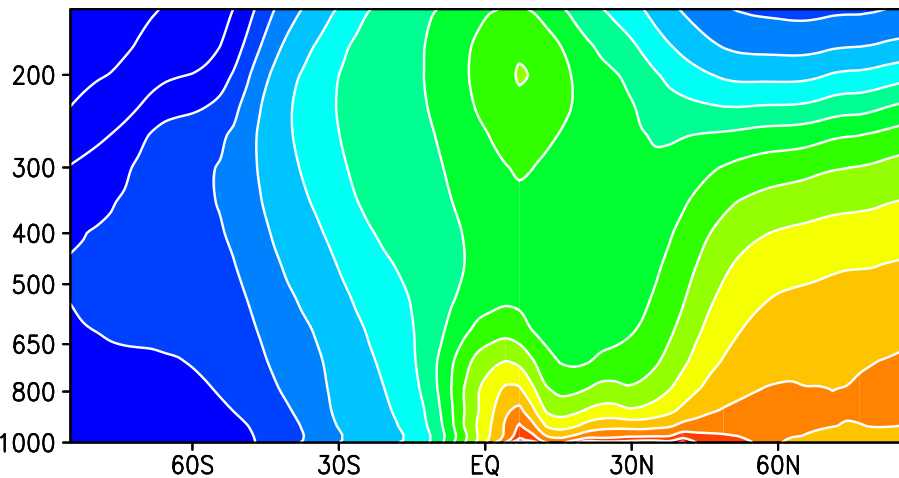　unit/IASC all meeting
» 4th DEGCR-all meeting
» 3rd DEGCR-all meeting

» Tropospheric
　Chemistry Reanalysis
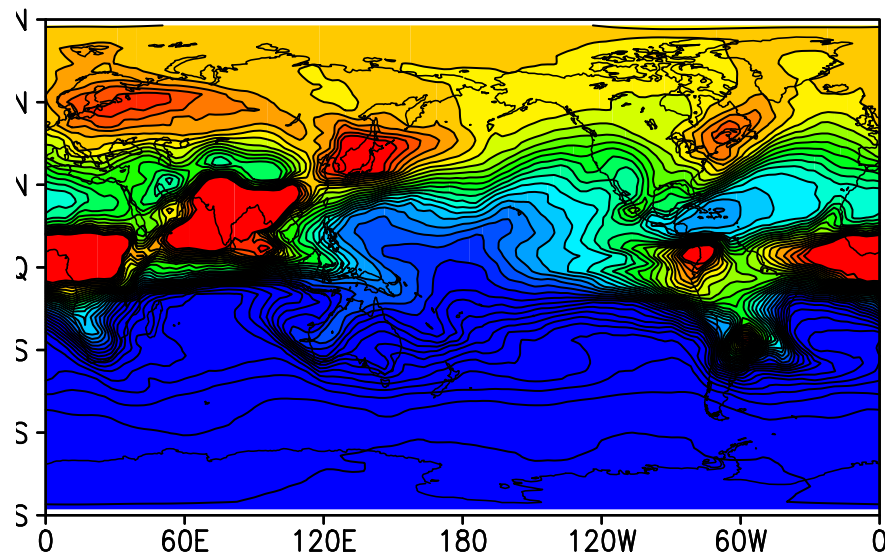　Data　NEW !

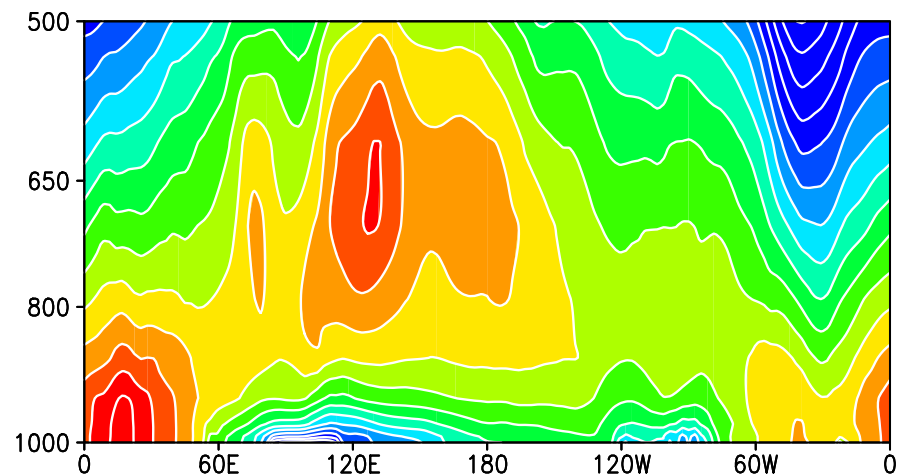» Global Chemical
　Weather Forecast
　System

一酸化炭素（CO）

3月

子午面分布

850hPa

経度分布 (75N)

排出量

Winter (average)

500 hPa

01JAN2005

800 hPa

01JAN2005

PBL origin region Ω_i	Free troposphere, $\dfrac{\bar{\bar{f}}_{ARC}(\Omega_i)}{\bar{\bar{f}}_{ARC}(\Omega_{MID})}$		Lower troposphere, $\dfrac{\bar{\bar{f}}_{ARC}(\Omega_i)}{\bar{\bar{f}}_{ARC}(\Omega_{MID})}$		Middle troposphere, $\dfrac{\bar{\bar{f}}_{ARC}(\Omega_i)}{\bar{\bar{f}}_{ARC}(\Omega_{MID})}$	
	DJF	JJA	DJF	JJA	DJF	JJA
WPAC	16%	9.1%	13%	10%	16%	9.0%
EPAC	26%	6.2%	25%	9.8%	26%	5.7%
ATL	20%	9.0%	15%	16%	21%	8.0%
NAM	13%	24%	16%	23%	12%	24%
EUR	13%	12%	20%	13%	12%	13%
ASI	12%	40%	12%	29%	12%	41%

Winter

500 hPa

01JAN2005

800 hPa

01JAN2005

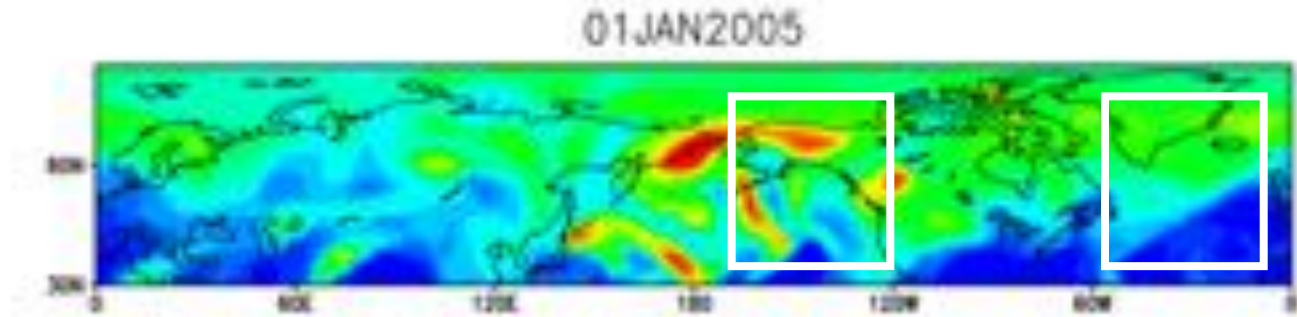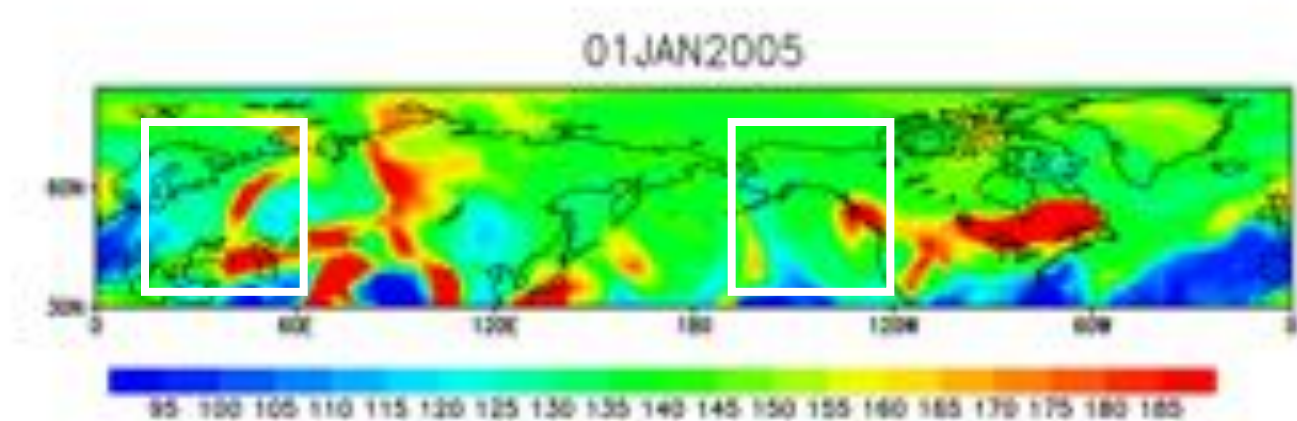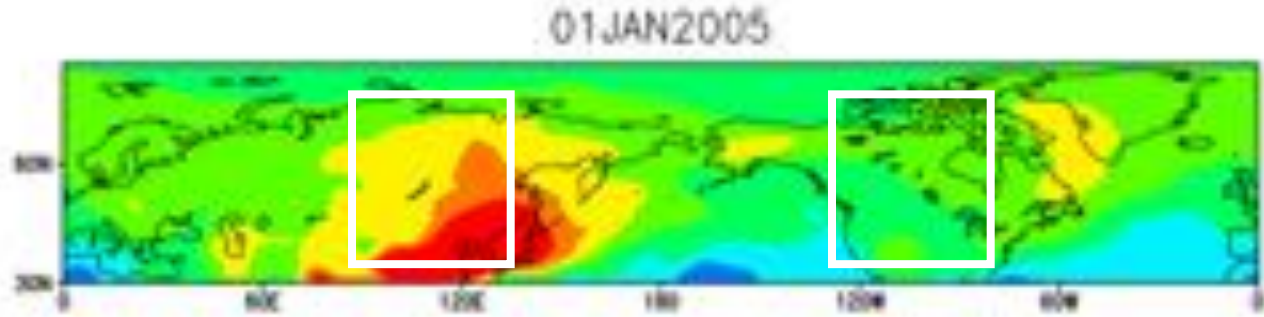95 100 105 110 115 120 125 130 135 140 145 150 155 160 165 170 175 180 185

PBL origin region Ω_i	Free troposphere, $\dfrac{\bar{f}_{ARC}(\Omega_i)}{\bar{f}_{ARC}(\Omega_{MID})}$		Lower troposphere, $\dfrac{\bar{f}_{ARC}(\Omega_i)}{\bar{f}_{ARC}(\Omega_{MID})}$		Middle troposphere, $\dfrac{\bar{f}_{ARC}(\Omega_i)}{\bar{f}_{ARC}(\Omega_{MID})}$	
	DJF	JJA	DJF	JJA	DJF	JJA
WPAC	16%	9.1%	13%	10%	16%	9.0%
EPAC	26%	6.2%	25%	9.8%	26%	5.7%
ATL	20%	9.0%	15%	16%	21%	8.0%
NAM	13%	24%	16%	23%	12%	24%
EUR	13%	12%	20%	13%	12%	13%
ASI	12%	40%	12%	29%	12%	41%

Summer (average)

500 hPa
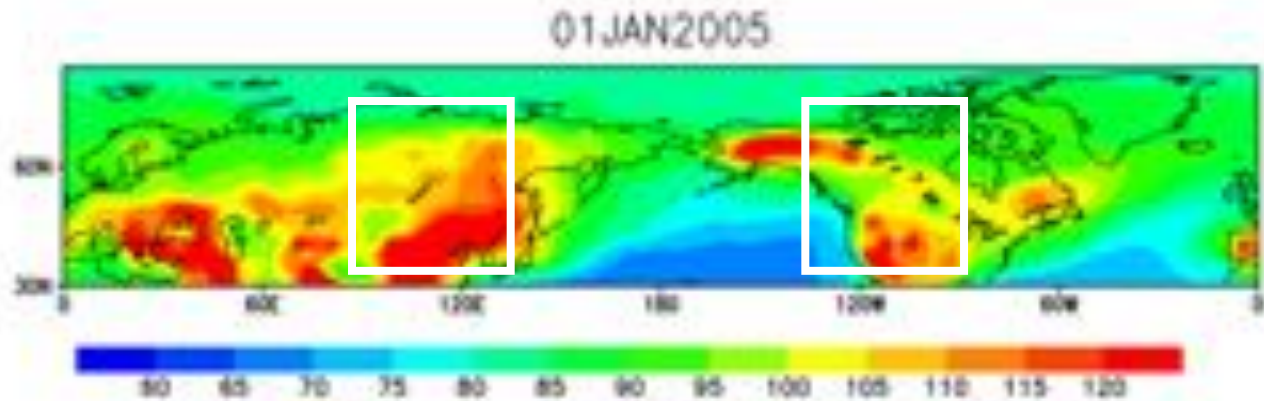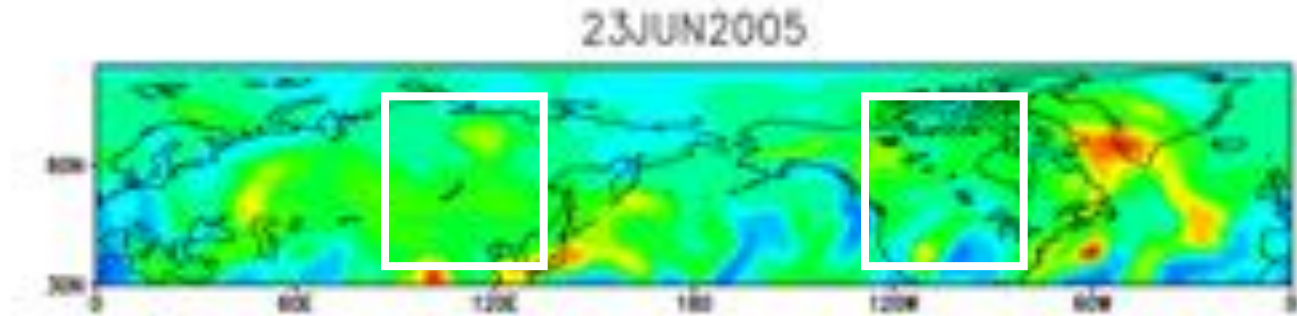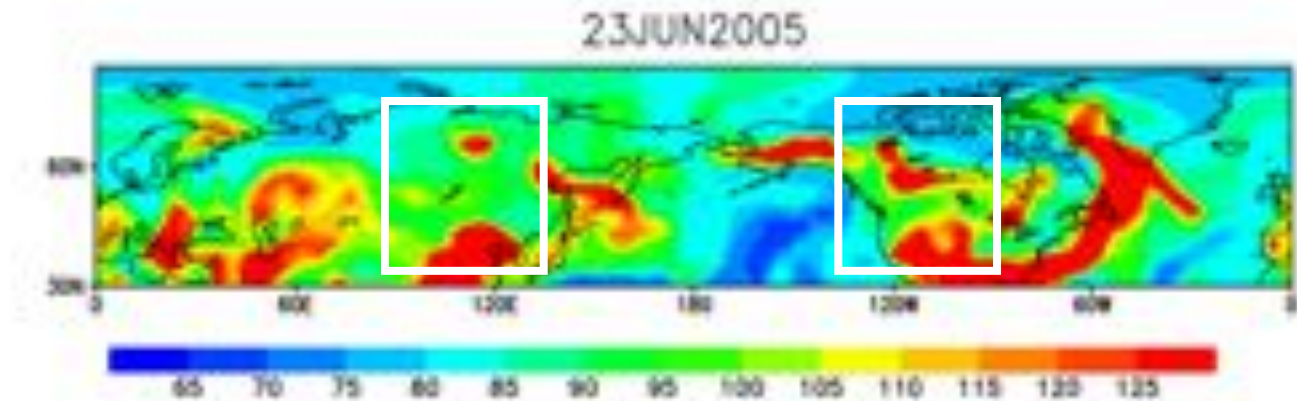

01JAN2005

800 hPa

01JAN2005

PBL origin region Ω_i	Free troposphere, $\dfrac{\bar{f}_{ARC}(\Omega_i)}{\bar{f}_{ARC}(\Omega_{MID})}$		Lower troposphere, $\dfrac{\bar{f}_{ARC}(\Omega_i)}{\bar{f}_{ARC}(\Omega_{MID})}$		Middle troposphere, $\dfrac{\bar{f}_{ARC}(\Omega_i)}{\bar{f}_{ARC}(\Omega_{MID})}$	
	DJF	JJA	DJF	JJA	DJF	JJA
WPAC	16%	9.1%	13%	10%	16%	9.0%
EPAC	26%	6.2%	25%	9.8%	26%	5.7%
ATL	20%	9.0%	15%	16%	21%	8.0%
NAM	13%	24%	16%	23%	12%	24%
EUR	13%	12%	20%	13%	12%	13%
ASI	12%	40%	12%	29%	12%	41%

Summer

500 hPa

23JUN2005

800 hPa

23JUN2005

PBL origin region Ω_i	Free troposphere, $\dfrac{\bar{f}_{\mathrm{ARC}}(\Omega_i)}{\bar{f}_{\mathrm{ARC}}(\Omega_{\mathrm{MID}})}$		Lower troposphere, $\dfrac{\bar{f}_{\mathrm{ARC}}(\Omega_i)}{\bar{f}_{\mathrm{ARC}}(\Omega_{\mathrm{MID}})}$		Middle troposphere, $\dfrac{\bar{f}_{\mathrm{ARC}}(\Omega_i)}{\bar{f}_{\mathrm{ARC}}(\Omega_{\mathrm{MID}})}$	
	DJF	JJA	DJF	JJA	DJF	JJA
WPAC	16%	9.1%	13%	10%	16%	9.0%
EPAC	26%	6.2%	25%	9.8%	26%	5.7%
ATL	20%	9.0%	15%	16%	21%	8.0%
NAM	13%	24%	16%	23%	12%	24%
EUR	13%	12%	20%	13%	12%	13%
ASI	12%	40%	12%	29%	12%	41%

今後の計画

・ 起源別解析（CTM）

・ 起源別解析（トラジェクトリー）